Constitutive activation of cellular immunity underlies the evolution of resistance to infection

Alexandre B. Leitão*, Ramesh Arunkumar*, Jonathan P. Day, Emma M. Geldman, Francis M. Jiggins

Department of Genetics, University of Cambridge, Cambridge, United Kingdom

* contributed equally

Abstract: Organisms rely on inducible and constitutive immune defences to combat infection. Constitutive immunity enables a rapid response to infection but may carry a cost for uninfected individuals, leading to the prediction that it will be favoured when infection rates are high. When we exposed populations of *Drosophila melanogaster* to intense parasitism by the parasitoid wasp *Leptopilina boulardi,* they evolved resistance by developing a more reactive cellular immune response. Using single-cell RNA sequencing, we found that immune-inducible genes had become constitutively upregulated. This was the result of resistant larvae differentiating precursors of specialized immune cells called lamellocytes that were previously only produced after infection. Therefore, populations evolved resistance by genetically hard-wiring an induced immune response to become constitutive.

One Sentence Summary: *Drosophila* populations that frequently encounter parasites have a constitutively activated immune response.

Main Text: A fundamental division within immune systems is between induced and constitutive immune defences. Constitutive immunity is always active, even in the absence of infection. For example, uninfected individuals produce natural antibodies (*1*), immune cells and antimicrobial peptides (AMPs) (*2*). In contrast, induced immune responses are triggered after infection, and frequently involve amplifying existing constitutive factors. This can include immune cells proliferating and differentiating, and the massive upregulation of AMPs and cyotoxic molecules (*2*). Constitutive immunity is fast, allowing hosts to avoid becoming infected altogether or rapidly clear infections. However, immune defences can be costly, diverting limited resources from other fitness-related traits (*3*) or damaging the host through immunopathology (*4*). While induced immune responses only incur these costs after infection, they are always present for constitutive immunity, even in the absence of infection. This trade-off between speed and cost is predicted to govern the allocation of host investment into constitutive and induced immunity (*5*, *6*). Theoretical models predict that the key parameter determining which type of defence should be favoured is the frequency that hosts are exposed to infection—more frequent exposure favours constitutive defences (*5*). In support of this, bacteria tend to evolve phage resistance by altering surface receptors when exposure is high and rely on induced CRISPR-Cas immunity when exposure is low (*7*). However, to our knowledge the key prediction that high rates of parasitism lead to induced immune responses becoming constitutively expressed has not been demonstrated.

40 To investigate these questions, we examined how the constitutive and induced
41 cellular immune defences of *Drosophila melanogaster* evolve under high parasite
42 pressure. Cellular immunity in *D. melanogaster* involves blood cells called
43 hemocytes, which play the equivalent role to leukocytes in vertebrates. In
44 uninfected larvae there are two morphological classes of hemocytes.
45 Plasmatocytes constitute the majority of cells and have diverse functions
46 including phagocytosis and AMP production (*8*). Crystal cells are a less abundant
47 specialized cell type that produces the prophenoloxidase molecules PPO1 and
48 PPO2, which are processed into enzymes required for the melanization of
49 parasites (*9*). Infection can trigger an induced response, where these cell types
50 proliferate, and cells called lamellocytes differentiate from plasmatocytes and
51 prohemocytes in the lymph gland (*8*). Lamellocytes are large flat cells with a
52 specialised role in killing large parasites like parasitic wasps (parasitoids). When
53 a parasitoid injects its egg into *D. melanogaster* larvae, plasmatocytes adhere to
54 the egg. Then, as lamellocytes differentiate they create additional cellular layers
55 known as a 'capsule'. Finally, the capsule is melanised by the activity of
56 phenoloxidases produced in crystal cells and lamellocytes (*9*). The melanin
57 physically encases the parasitoid and toxic by-products of the melanisation
58 reaction likely contribute to parasite killing (*10*).
59 There is substantial genetic variation in susceptibility to parasitoid infection
60 within *D. melanogaster* populations (*11*), and this is associated with differences
61 in hemocyte composition (*12*, *13*). Here, we used a combination of experimental
62 evolution with physiological assays and single-cell RNA sequencing to examine
63 how a high rate of parasitism by the parasitoid wasp *L. boulardi* affects
64 constitutive and induced immune defences.

65

66 **The evolution of resistance is associated with a more reactive immune**

67 **response**

68 To investigate the evolution of the cellular immune response, we allowed

69 genetically diverse populations of *D. melanogaster* to evolve under intense levels

70 of parasitism. We established an outbred population from 377 wild-caught *D.*

71 *melanogaster* females, and used this to found six experimental populations that

72 were maintained at population sizes of 200 flies. In three of these populations,

73 larvae were infected every generation, and flies that survived by encapsulating

74 and melanising the wasp were used to establish the next generation (High

75 Parasitism populations). The other three populations were maintained in the

76 same conditions but without infection (No Parasitism populations). In line with

77 previous studies (*12*, *14*), the High Parasitism populations increased in

78 resistance over the generations (Fig. 1A, Selection regime x Generation: χ^2=

79 91.41, d.f.= 1, $p<10^{-15}$). After 33 generations, a mean of 76% of flies survived

80 infection in the High Parasitism populations, compared to 10% in the No

81 Parasitism controls.

82

83 As populations evolved resistance, they melanised parasitoids at a higher rate

84 (Fig. 1A). This could result from increased basal reactivity of the encapsulation

85 immune response, or because the flies are evolving to escape the effects of

86 immunosuppressive molecules produced by the parasite. To distinguish these

87 possibilities, we measured the ability of each population to react to an inert

88 object. When a small volume of paraffin oil is injected into the larval haemocoel,

89 it remains as a sphere and can be encapsulated (*15*). Populations that evolved

without parasitism show a very limited reaction to the oil droplets (Fig. 1B). In contrast, approximately half of larvae from selected populations encapsulate the oil droplet (Fig. 1B; Selection Regime: $F_{1,4}$=24.53, p=0.008). Therefore, high levels of parasitism led to the cellular immune system evolving a more reactive encapsulation response.

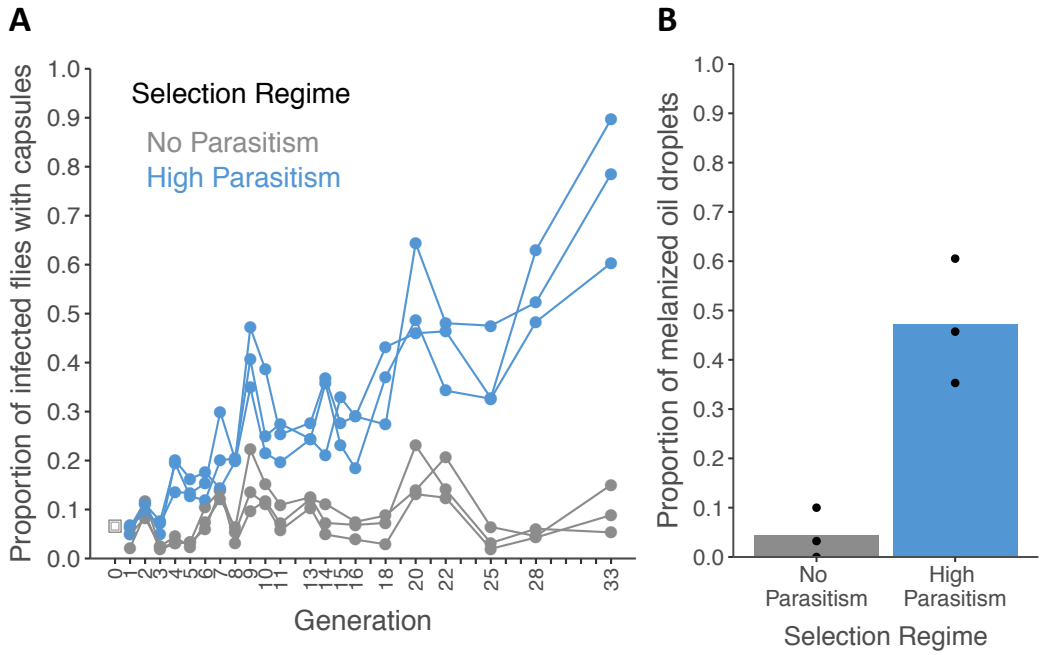

Figure 1 Encapsulation rate during selection for parasitoid resistance. (A) The proportion of infected larvae that gave rise to adult flies with visible capsules. An outbred population of *D. melanogaster* (source, grey square) was used to found six populations that were parasitized every generation with *L. boulardi* (blue) or maintained without infection (grey). (B) The proportion of larvae encapsulating oil droplets at generation 33. Dots represent the proportion of larvae in replicate populations and bars represent the mean per selection regime.

Constitutive upregulation of immune-induced genes

Underlying induced immune responses is a transcriptional response to infection, so we examined how the hemocyte transcriptome altered in populations that evolved under high levels of parasitism. Initially, we pooled the data from

108 scRNA-seq to investigate global changes in hemocyte gene expression. As
109 expected, 48 hours post infection there was a strong transcriptional response to
110 infection (Fig. 2A, X axis; Data S1). Strikingly similar transcriptional changes
111 occurred in uninfected flies that had evolved under high rates of parasitism for
112 26 generations (Fig. 2A, Y axis; Data S1). Taking the 173 genes that had at least a
113 50% change in transcript levels after infection or selection, in every case the
114 direction of change was the same after infection and adaptation to high
115 parasitism (Fig. 2A; Data S1). We verified that the evolved response mimicked
116 the induced response by using quantitative PCR (qPCR) to measure the
117 expression of the lamellocyte marker *atilla* and the anti-parasitoid effector gene
118 *PPO3* (Fig. S1). Again, we found that high rates of parasitism led to these
119 immune-induced genes becoming constitutively upregulated. Therefore, as
120 populations evolved resistance, the induced transcriptional response to infection
121 has become genetically hard-wired and constitutive.

122

123 We took the same approach to examine how the induced transcriptional
124 response to infection changed as populations evolved resistance. We found that
125 the transcriptional response to infection involved the same genes in the different
126 populations (Fig. 2B). However, the magnitude of the changes in gene expression
127 was substantially less in populations that had evolved under high parasite
128 pressure (Fig. 2B). Therefore, the increase in constitutive gene expression has
129 been matched by a decrease in induced expression. Again, this was verified by
130 qPCR (Fig. S1). Combining the constitutive and induced changes in gene
131 expression, the hemocyte transcriptome after infection is similar in the

132 populations that evolved under high levels of parasitism and the controls (Fig.
133 2C). Therefore, an induced response has become genetically fixed, as opposed to
134 selection leading to a greater total response.

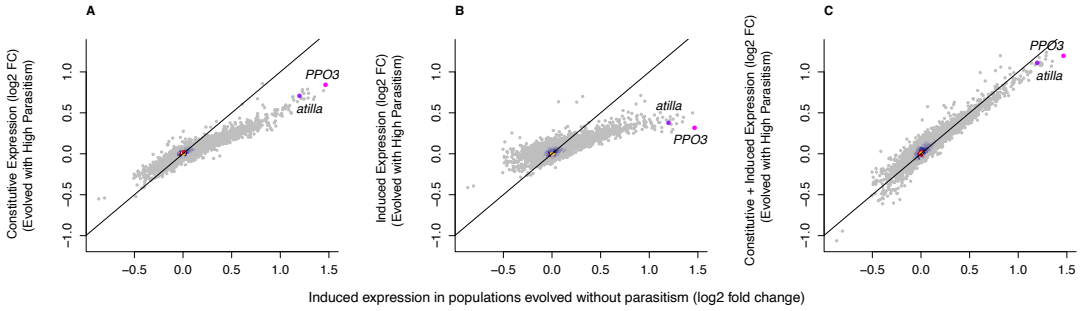

135 **Figure 2. Changes in gene expression following selection for resistance and**
136 **parasitoid infection.** (A) Constitutive gene expression following 26 generations of
137 selection for resistance to the parasitoid wasp *L. boulardi* (y-axis). (B) The induced
138 change in gene expression following infection with *L. boulardi* in populations selected for
139 resistance (y-axis). (C) The combined induced and constitutive change in gene
140 expression following selection for resistance and infection (y-axis). All are compared to
141 the change in gene expression following infection in populations maintained without
142 parasitoid infection (x-axis). The black diagonal indicates the 1:1 line. The genes *atilla*
143 and *PPO3* are highlighted. Colour represents the density of overlain points. Relative
144 expression is expressed as $\log_2$(fold change).

145

146 **scRNA-seq reveals novel hemocyte types**

147 The global changes in hemocyte transcriptomes could result from a change in the
148 relative proportion of cell types in the hemocyte population, or from a shift in
149 gene expression within existing cell types. The three classical *Drosophila*
150 hemocyte types were originally defined morphologically, but emerging single
151 cell transcriptomic data suggests that *Drosophila* hemocyte populations are more

152 complex than this (*16–19*). Excluding cells that did not express the pan-hemocyte
153 markers *Hemese* or *Serpent* (*20*, *21*), we grouped 19,344 larval hemocytes into
154 nine clusters based on their transcriptomes (Fig. 3A). Neither infection nor
155 selection leads to the appearance of new cell states (Fig. 3B).

156 We identified two large clusters of plasmatocytes. The largest was PLASM1,
157 which we classify as the cycling plasmatocyte state as it had the greatest number
158 of replicating cells in the G2M or S phase (Fig. S2). The 5,712 cells in this cluster
159 had high expression of genes associated with plasmatocytes (*Col4a1*, *Pxn*, *eater*,
160 *Hml*, *NimC1* -(*21*)) and actively replicating cells (*stg* – (*22*), *polo* – (*23*)and *scra* –
161 (*24*)) (Fig. S3). The next largest cluster, PLASM2, contained 2,874 plasmatocytes
162 that were enriched for the genes encoding rRNA (Fig. S4) or involved in the
163 ribosome biogenesis (Data S3). There were two smaller plasmatocyte clusters.
164 The AMP cluster contained 196 cells with elevated expression of genes encoding
165 antimicrobial and antifungal peptides, including *Drs*, *Mtk* and *CecA1* (Lemaitre
166 and Hoffmann 2007, Fig. S4; Data S3). The MET cluster contained 283 cells with
167 high expression of the heat shock proteins *Hsp24* and *Hsp27* and genes involved
168 in organic acid metabolism (Fig. S4; Data S3). The crystal cells formed a single
169 cluster of 906 cells (Fig. S6). Three clusters of cells, LAM 1, 2 and 3, had elevated
170 expression of one or more lamellocyte marker genes (*21*) (Fig. S5) and contained
171 1,260, 5,104 and 3,000 cells respectively.

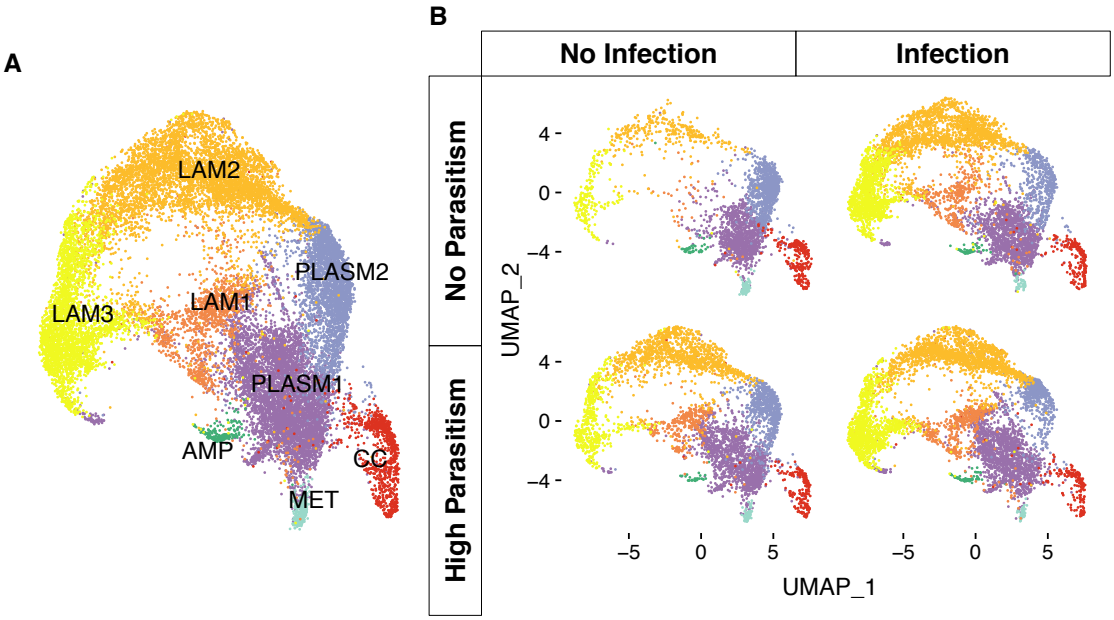

172 **Figure 3. Cell states of *Drosophila melanogaster* larval hemocytes.** Two-dimensional
173 UMAP projections and cell state classification. (A) All 19,344 cells combined. PLASM:
174 plasmatocytes; MET: metabolic plasmatocyte cluster; AMP: antimicrobial peptide
175 plasmatocyte cluster; LAM: lamellocytes; CC: crystal cells. (B) Cells from populations that
176 had undergone 26 generations of selection with no parasitism (top panels) or high
177 parasitism (bottom panels), and were either uninfected (left panels) or 48 hours post
178 infection (right panels). 64-333 million reads were sequenced in each of the eight 10X
179 libraries that we generated (Data S2). The number of cells detected per library ranged
180 from 787 to 3,463 (Fig. S6).

181

182 **Inducible cell states are present constitutively in resistant populations**

183 Lamellocytes are key effector cells in the anti-parasitoid immune response. In
184 populations that evolved without exposure to parasitoids, infection resulted in a
185 large increase in the number of cells in all three lamellocyte clusters (LAM1-3,
186 Fig. 3B and 4A). In populations that evolved under high levels of parasitism, this
187 inducible response become constitutive, with uninfected larvae having 3-5 fold
188 more cells in LAM1 and 2 (Fig. 4A). However, this was matched by a reduction in

189 the induced response, so the final number of cells in these clusters after infection
190 was similar regardless of whether the populations had adapted to high or low
191 parasitism rates (Fig. 4A). These results held when replicate populations were
192 analyzed separately (Fig. S7A, B) or when the number of cells in each library
193 were down-sampled to match the library with the least number of cells (Fig.
194 S7C). Therefore, high infection rates led to the inducible differentiation of
195 specialised immune cells becoming genetically fixed.

196 To investigate the developmental origins of this change, we reconstructed the
197 pathway by which plasmatocytes differentiate into mature lamellocytes. By
198 subclustering the cells and ordering them along a pseudotemporal scale, we
199 found a single lineage starting from the self-cycling plasmatocytes (PLASM1) and
200 ending in LAM3 (Figs. 4B). Along this lineage there was a decrease in cell
201 replication, with the largest fraction of cells in the G2M and S phase in PLASM1
202 and the largest fraction in G1 in LAM3 (Fig. S8). Importantly, controlling for the
203 effects of cell cycle had a negligible impact on the clustering (Table S1) and the
204 trajectory of lamellocyte differentiation (Fig. S9). The expression of the effector
205 gene *PPO3,* the lamellocyte marker *atilla* and other marker genes all increased as
206 cells progressed along this trajectory (Fig. 4C, 4D and S10, Data S4). On the other
207 hand, genes involved in extracellular matrix organization—a house-keeping
208 function of plasmatocytes (*25*, *26*)—were down-regulated as cells differentiated
209 (Data S5). Together, these results suggest that LAM1 cells are immature
210 lamellocytes, while LAM3 cells are mature lamellocytes. Comparing our
211 populations, the inducible production of LAM1 cells has become entirely
212 constitutive in the populations evolved under high rates of parasitism, while
213 much of the LAM3 response remains inducible. This suggests that high infection

214 rates result in the cellular immune response becoming 'primed' by constitutively

215 producing the precursors of the cells required for parasite killing.

216

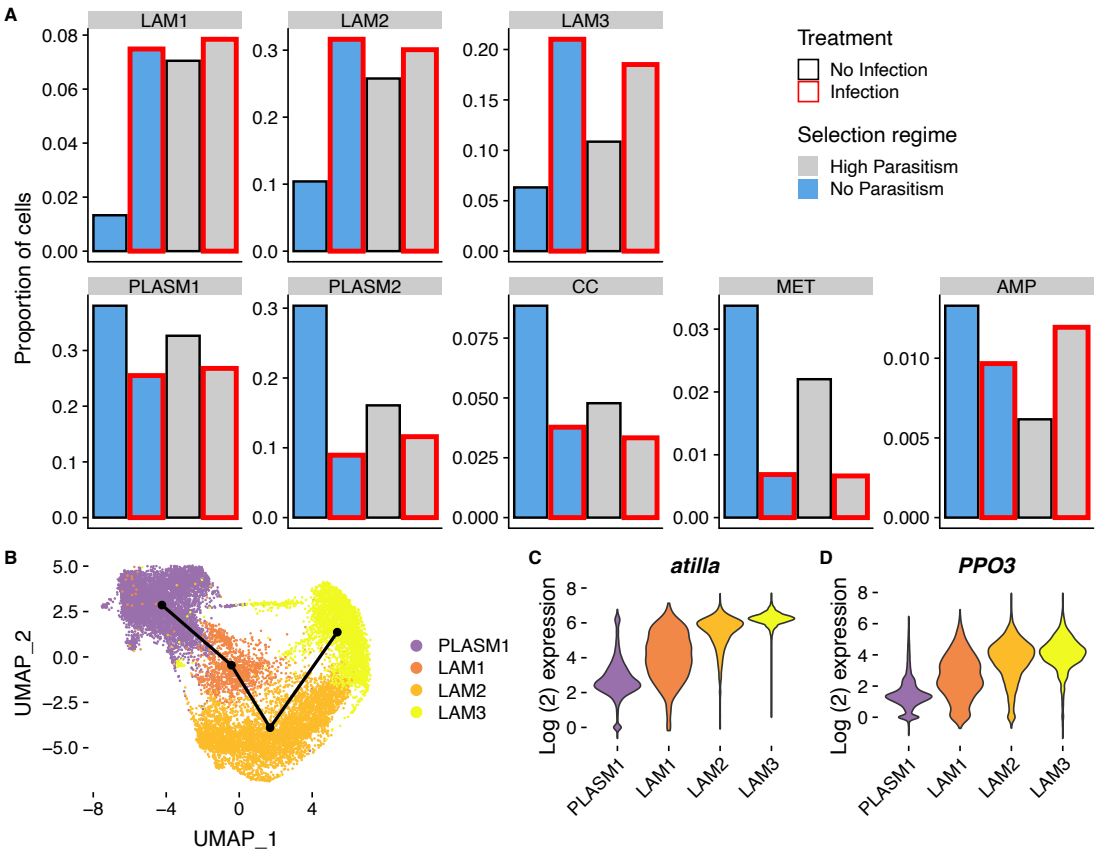

217

218 **Figure 4. Changes in cell state following infection and adaptation to high rates of**

219 **parasitism.** (A) Proportion of different cell states after infection and selection. (B)

220 Trajectory of lamellocyte differentiation. Plasmatocyte progenitors and lamellocytes

221 were subclustered, the trajectories inferred from multi-dimensional principle

222 components analysis, and the lineage projected onto the two-dimensional UMAP plot. (C-

223 D) Log_2 expression levels of *atilla* and *PPO3*. Relative expression levels were estimated

224 from normalized and scaled unique molecular identifier counts.

225

226

227 **Morphological differentiation of immune cells remains an inducible**
228 **response**

229 Lamellocytes are classically defined morphologically as large flattened cells. As
230 expected, the proportion of morphologically identifiable lamellocytes increased
231 after infection (Figs 5A and Fig. S11A; Treatment: χ^2= 48.14, d.f= 1, p=3.97x10^{-}
232 ^{12}). However, in contrast to our analysis of single cell transcriptomes, there was
233 little difference between selection regimes in either the induced or constitutive
234 proportion of these cells (Figs 5A and Fig. S11A; Selection regime x Treatment:
235 χ^2= 0.16, d.f= 1, p=0.69; Selection regime: χ^2= 0.41, d.f= 1, p=0.52). This suggests
236 that while the transcriptional state of cells has been constitutively activated, the
237 change in cell morphology remains an inducible response. To test this
238 hypothesis, we used microscopy to measure both cell morphology and, as a
239 marker of the transcriptional state of the cells, *atilla* expression (Fig. S12). In line
240 with our scRNAseq data, both infection and adaptation to high parasitism rates
241 increases the proportion of *atilla* positive cells (Fig. 5C; Selection Regime x
242 Treatment: F=16.3, d.f=1,8, p=0.004). However, among the *atilla* positive cells,
243 infection had a large effect on cell size (Fig. 5C; Treatment: F=31.8, d.f.=1,7,
244 p=0.0008), while selection had a small effect (Fig. 5C; Selection Regime: F=7.2,
245 d.f.=1,7, p=0.03). Therefore, while selection has resulted in the constitutive
246 transcriptional activation of cells, changes in cell morphology remain largely an
247 inducible response.

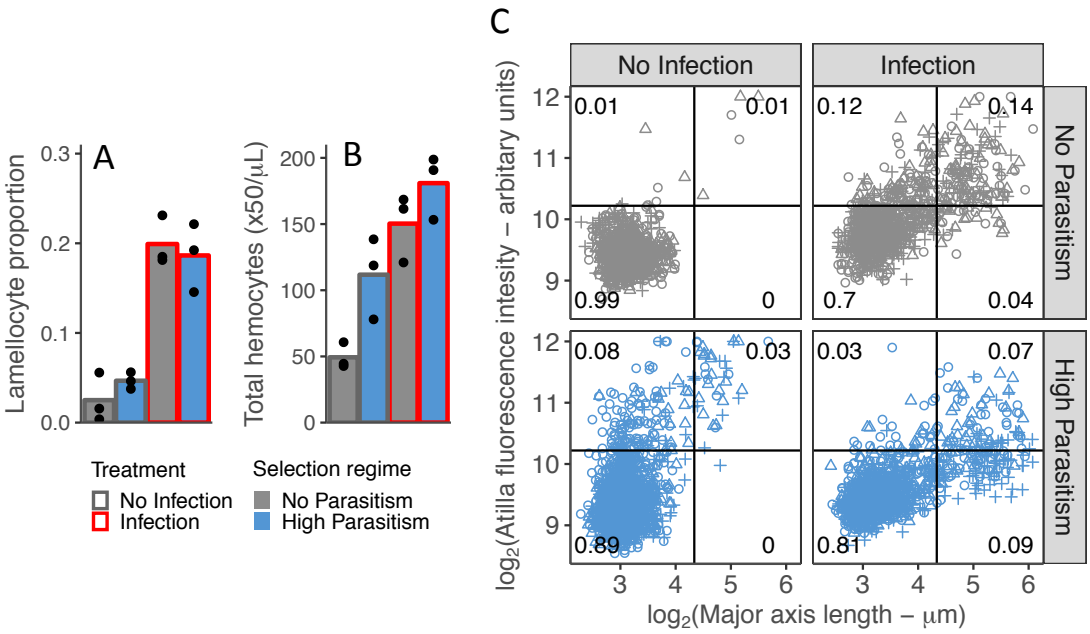

Figure 5. Changes in the morphology and number of cells following infection and adaptation to high parasitism rates. (A) The proportion hemocytes that were morphologically identified as lamellocytes and (B) the concentration of total circulating hemocytes in no infection conditions (grey outline) and 48 hours post infection (red outlines). Samples were collected from populations that evolved 34 generation with high parasitism (blue bars) or no parasitism (grey bars) (C) Cell size and *atilla* expression. The expression of *atilla* was measured as the fluorescence intensity resulting from immunohistochemistry staining. Cell size was measured along the major axis. Replicated populations from each selection regime are represented by different symbols and the proportion of cells in each quarter of the plot is shown.

In addition to the change in the transcriptional state of cells, we found that the populations maintained under strong parasite pressure evolved a constitutive increase in the absolute number of hemocytes in circulation (Fig. 5B and Fig. S11B, Selection regime: χ^2= 22.37, d.f= 1, p=2.25x10^{-6}). This supports results from previous selection experiments (*13*, *27*) and comparative analyses (*28*), and is another aspect of the induced response that has become constitutive.

266 **Conclusions**

267 Our results provide support for the hypothesis that natural selection favours
268 constitutive defences when infection is common (*5–7*) by demonstrating that an
269 inducible immune response becomes constitutive when populations frequently
270 encounter a parasite. The induced immune response to parasitoids relies on the
271 differentiation of lamellocytes from embryonic-derived plasmatocytes, lymph
272 gland prohemocytes (*8*) and lymph gland plasmatocytes (*18*). Evidence for
273 immature lamellocytes has previously come from patterns of marker gene
274 expression (*29*, *30*) and recent scRNAseq data (*17*, *19*). Our results show that
275 *Drosophila* populations evolve to produce these cells constitutively if they are
276 frequently exposed to infection. However, this change in the transcriptional state
277 of cells was not accompanied by morphological differentiation. Genes involved in
278 cytoskeleton dynamics such as *βTub60D* and *shot* are among the genes with the
279 greatest increases in expression as lamellocytes differentiate (Fig. S10, Data S4)
280 and these may be required for the final step of changing cell shape (*31*).
281 Together, our results suggest populations that adapt to high parasitism rates
282 have their cellular immune defences in a state of readiness, with the final step of
283 cell differentiation remaining an inducible response.
284
285 Evolving resistance to parasitoid wasps is costly in *Drosophila* (*12*, *14*, *32*), so
286 inducible immunity may be an adaptation that allows uninfected individuals to
287 avoid this cost under low parasitism conditions. The physiological mechanism
288 that causes the cost is unknown. It is possible that the differentiation of
289 immature lamellocytes diverts resources from other fitness related traits.
290 Lamellocyte differentiation is energy-demanding and results in the increased

291 expression of glycolysis genes in hemocytes after infection (*3*). This cost may be
292 borne by uninfected flies in our resistant populations, as we found that genes
293 involved in trehalose uptake and catabolism (*33*), *Trehalase* and *Tret1-1*, are
294 upregulated by both infection and selection (Fig. S13). Another possibility is that
295 a more reactive cellular immune response may increase the effects of
296 immunopathology.
297
298 After infection, whether the host or parasitoid survives is a race between the
299 parasitoid development and the formation of a cellular capsule by the immune
300 system (*34*). Constitutive differentiation of immature lamellocytes may allow
301 lamellocytes to be produced more rapidly upon infection. Furthermore, cytotoxic
302 molecules could be more readily available. This is supported by an increase in
303 the constitutive expression of *PPO3* in populations adapted to high rates of
304 parasitism. *PPO3* encodes a intracellular prophenoloxidase that, when active, is
305 responsible for the melanization of lamellocytes (*9*). Along with the increase in
306 the total number of hemocytes, the constitutive activation of the cellular immune
307 response likely explains the greatly increased resistance of populations adapted
308 to high rates of parasitism.
309
310 **References and Notes:**
311
312 1. H. P. Savage, V. M. Yenson, S. S. Sawhney, B. J. Mousseau, F. E. Lund, N.
313 Baumgarth, Blimp-1-dependent and -independent natural antibody
314 production by B-1 and B-1-derived plasma cells. *J. Exp. Med.* **214**, 2777–
315 2794 (2017).

316 2. B. Lemaitre, J. Hoffmann, The host defense of Drosophila melanogaster.
317 *Annu. Rev. Immunol.* **25**, 697–743 (2007).

318 3. A. Bajgar, K. Kucerova, L. Jonatova, A. Tomcala, I. Schneedorferova, J.
319 Okrouhlik, T. Dolezal, Extracellular Adenosine Mediates a Systemic
320 Metabolic Switch during Immune Response. *PLoS Biol.* **13**, 1–23 (2015).

321 4. A. L. Graham, J. E. Allen, A. F. Read, Evolutionary causes and consequences
322 of immunopathology. *Annu. Rev. Ecol. Evol. Syst.* **36**, 373–397 (2005).

323 5. E. Shudo, Y. Iwasa, Inducible defense against pathogens and parasites:
324 Optimal choice among multiple options. *J. Theor. Biol.* **209**, 233–247
325 (2001).

326 6. M. Boots, A. Best, The evolution of constitutive and induced defences to
327 infectious disease. *Proc. R. Soc. B Biol. Sci.* **285** (2018),
328 doi:10.1098/rspb.2018.0658.

329 7. E. R. Westra, S. Van houte, S. Oyesiku-Blakemore, B. Makin, J. M.
330 Broniewski, A. Best, J. Bondy-Denomy, A. Davidson, M. Boots, A. Buckling,
331 Parasite exposure drives selective evolution of constitutive versus
332 inducible defense. *Curr. Biol.* **25**, 1043–1049 (2015).

333 8. V. Honti, G. Csordás, É. Kurucz, R. Márkus, I. Andó, The cell-mediated
334 immunity of Drosophila melanogaster: hemocyte lineages, immune
335 compartments, microanatomy and regulation. *Dev. Comp. Immunol.* **42**,
336 47–56 (2014).

337 9. J. P. Dudzic, S. Kondo, R. Ueda, C. M. Bergman, B. Lemaitre, Drosophila
338 innate immunity: regional and functional specialization of

339 prophenoloxidases. *BMC Biol.* **13**, 81–97 (2015).

340 10. A. J. Nappi, M. Poirié, Y. Carton, in *Advances in Parasitology* (2009), pp. 99–
341 121.

342 11. A. R. Kraaijeveld, H. C. J. Godfray, Geographic Patterns in the Evolution of
343 Resistance and Virulence in Drosophila and Its Parasitoids. *Am. Nat.* **153**,
344 S61–S74 (1999).

345 12. J. E. McGonigle, A. B. Leitão, S. Ommeslag, S. Smith, J. P. Day, F. M. Jiggins,
346 Parallel and costly changes to cellular immunity underlie the evolution of
347 parasitoid resistance in three Drosophila species. *PLoS Pathog.* **13** (2017),
348 doi:10.1371/journal.ppat.1006683.

349 13. A. R. Kraaijeveld, E. C. Limentani, H. C. Godfray, Basis of the trade-off
350 between parasitoid resistance and larval competitive ability in Drosophila
351 melanogaster. *Proc. Biol. Sci.* **268**, 259–61 (2001).

352 14. M. D. Fellowes, A. R. Kraaijeveld, H. C. Godfray, Trade-off associated with
353 selection for increased ability to resist parasitoid attack in Drosophila
354 melanogaster. *Proc Biol Sci*. **265**, 1553–1558 (1998).

355 15. S. Havard, P. Eslin, G. Prévost, G. Doury, Encapsulation ability: Are all
356 *Drosophila* species equally armed? An investigation in the *obscura* group.
357 *Can. J. Zool.* **87**, 635–641 (2009).

358 16. Y. Fu, X. Huang, P. Zhang, J. Van De Leemput, Z. Han, Single-cell RNA
359 sequencing identifies novel cell types in Drosophila blood. *J. Genet.*
360 *Genomics* (2020), doi:10.1016/j.jgg.2020.02.004.

361 17. S. Gopal Tattikota, Y. Hu, Y. Liu, B. Cho, V. Barrera, M. Steinbaugh, S.-H.

362 Yoon, A. Comjean, F. Li, F. Dervis, R.-J. Hung, J.-W. Nam, S. H. Sui, J. Shim, N.
363 Perrimon, A single-cell survey of Drosophila blood (2019),
364 doi:10.1101/2019.12.20.884999.

365 18. B. Cho, Single-cell transcriptome maps of myeloid blood cell lineages in
366 Drosophila. *bioRxiv* (2020).

367 19. P. B. Cattenoz, R. Sakr, A. Pavlidaki, C. Delaporte, A. Riba, N. Molina, N.
368 Hariharan, T. Mukherjee, A. Giangrande, Temporal specificity and
369 heterogeneity of Drosophila immune cells . *EMBO J.*, 1–25 (2020).

370 20. R. B. V. Vivancos, A. Giangrande, glide/gcmIs Expressed and Required in
371 the Scavenger Cell Lineage. *Dev. Biol.* **191**, 118–130 (1997).

372 21. U. Banerjee, J. R. Girard, L. M. Goins, C. M. Spratford, *Drosophila* as a Genetic
373 Model for Hematopoiesis. *Genetics*. **211**, 367–417 (2019).

374 22. B. A. Edgar, P. H. O'Farrell, The three postblastoderm cell cycles of
375 Drosophila embryogenesis are regulated in G2 by string. *Cell*. **62**, 469–480
376 (1990).

377 23. D. M. Glover, Polo kinase and progression through M phase in Drosophila:
378 a perspective from the spindle poles. *Oncogene*. **24**, 230–237 (2005).

379 24. K. Oegema, M. S. Savoian, T. J. Mitchison, C. M. Field, Functional Analysis of
380 a Human Homologue of the Drosophila Actin Binding Protein Anillin
381 Suggests a Role in Cytokinesis. *J. Cell Biol.* **150**, 539–552 (2000).

382 25. B. Olofsson, D. T. Page, Condensation of the central nervous system in
383 embryonic Drosophila is inhibited by blocking hemocyte migration or
384 neural activity. *Dev. Biol.* **279**, 233–243 (2005).

385 26. S. Bunt, C. Hooley, N. Hu, C. Scahill, H. Weavers, H. Skaer, Hemocyte-
386 Secreted Type IV Collagen Enhances BMP Signaling to Guide Renal Tubule
387 Morphogenesis in Drosophila. *Dev. Cell*. **19**, 296–306 (2010).

388 27. J. E. Mcgonigle, A. B. Leitão, S. Ommeslag, S. Smith, P. Day, F. M. Jiggins,
389 Parallel and costly changes to cellular immunity underlie the evolution of
390 parasitoid resistance in three Drosophila species. *PLoS Pathog.* **13(10)**, 1–
391 20 (2017).

392 28. P. Eslin, G. Prevost, Hemocyte load and immune resistance to Asobara
393 tabida are correlated in species of the Drosophila melanogaster subgroup.
394 *J. Insect Physiol.* **44**, 807–816 (1998).

395 29. V. Honti, G. Csordás, R. Márkus, E. Kurucz, F. Jankovics, I. Andó, Cell lineage
396 tracing reveals the plasticity of the hemocyte lineages and of the
397 hematopoietic compartments in Drosophila melanogaster. *Mol. Immunol.*
398 **47**, 1997–2004 (2010).

399 30. I. Anderl, L. Vesala, T. O. Ihalainen, L. M. Vanha-aho, I. Andó, M. Rämet, D.
400 Hultmark, Transdifferentiation and Proliferation in Two Distinct
401 Hemocyte Lineages in Drosophila melanogaster Larvae after Wasp
402 Infection. *PLoS Pathog.* **12**, 1–34 (2016).

403 31. T. M. Rizki, R. M. Rizki, Parasitoid-induced cellular immune deficiency in
404 Drosophila. *Ann. N. Y. Acad. Sci.* **712**, 178–94 (1994).

405 32. A. R. Kraaijeveld, H. C. Godfray, Trade-off between parasitoid resistance
406 and larval competitive ability in Drosophila melanogaster. *Nature*. **389**,
407 278–280 (1997).

408 33. J. Mattila, V. Hietakangas, Regulation of carbohydrate energy metabolism
409 in Drosophila melanogaster. *Genetics* (2017),
410 doi:10.1534/genetics.117.199885.

411 34. C. Kim-Jo, J. L. Gatti, M. Poirié, Drosophila cellular immunity against
412 parasitoid wasps: A complex and time-dependent process. *Front. Physiol.*
413 **10** (2019), doi:10.3389/fphys.2019.00603.

414

415 **Acknowledgements:** The Genomics Core Facility at Cancer Research UK
416 Cambridge Institute, G. Raddi and S. Tattikota provided protocols for the
417 scRNAseq. **Funding:** This work was funded by Natural Environment Research
418 Council grant NE/P00184X/1 to FJ and AL, an EMBO Postdoctoral Fellowship to
419 AL (ALT-1556) and a Natural Sciences and Engineering Research Council of
420 Canada Postdoctoral Fellowship (PDF-516634-2018, Committee: 187) to RA.
421 **Competing Interests:** None. **Author Contributions:** AL, RA and FMJ designed
422 the study and wrote the paper with input from the other authors. AL, JD and EG
423 performed the *Drosophila* work. AL and JD generated the sequencing data. RA
424 analysed the sequence data. **Data and materials availability:** Unprocessed
425 single cell sequence reads were deposited in the Sequence Read Archive
426 (accession: SRP256887, Bioproject: PRJNA625925). Cell count matrices for all
427 detected genes, cluster identities and processed scRNA-seq results were
428 deposited into Gene Expression Omnibus (accession: GSE148826). The R script
429 used to analyze the scRNA-seq data is available on Github (Repository:
430 dmel_scRNA_hemocyte).